Journal of Sound and Vibration (2002) **251**(4), 717–740
doi:10.1006/jsvi.2001.3986, available online at http://www.idealibrary.com on IDEAL®

HYDROELASTIC COUPLED VIBRATIONS IN A CYLINDRICAL CONTAINER WITH A MEMBRANE BOTTOM, CONTAINING LIQUID WITH SURFACE TENSION

M. CHIBA AND H. WATANABE

Department of Mechanical Engineering, Faculty of Engineering, Iwate University, 4-3-5 *Ueda, Morioka* 020-8551, *Japan. E-mail: mchiba@iwate-u.ac.jp*

AND

H. F. BAUER

Institut für Raumfahrttechnik, Universität der Bundeswehr München, 85577 *Neubiberg, Germany*

(*Received* 22 *November* 2000, *and in final form* 30 *July* 2001)

A linear free hydroelastic vibration analysis of a frictionless liquid with a free surface contained in a cylindrical tank with a flexible bottom has been performed. The side-wall has been treated as rigid and the effect of surface tension taken into consideration. The container bottom was treated as a membrane, while for the free liquid surface the effect of two contact line conditions has been investigated. One edge condition was that of a slipping contact line, while the other one treated the contact line as fixed, i.e., an anchored edge. The vibration characteristics of a membrane–liquid coupled system have been investigated for various system parameters, i.e., membrane tension parameter $\bar{T}$, liquid surface tension parameter $\bar{\sigma}$, material density parameter $\bar{\rho}$, liquid height ratio ℓ_0 and vibration mode numbers m and n. The degree of coupling between a membrane and a liquid was represented with vibration mode diagrams as well as with frequency diagrams. For axisymmetric coupled vibrations with anchored edge condition, vibration mode exchanging of both a membrane and liquid free surface with membrane bottom tension parameter $\bar{T}$ has been investigated. An interesting phenomenon which is only observed for a flexible bottom container and an anchored edge free surface condition is presented.

© 2002 Elsevier Science Ltd.

1. INTRODUCTION

Structure–liquid coupling is one of the interesting fields of coupled dynamic systems in complex engineering problems. One of the most popular structural configurations in the industrial or engineering field is a cylindrical tank filled with liquid, i.e., liquid storage tanks, fuel vessels, various kinds of pressure vessels, etc. For a safe design of such structures, vibration characteristics of a cylindrical shell filled with liquid have been investigated for years, theoretically and experimentally.

In the present study, we focus on a cylindrical container with a rigid side-wall and a flexible bottom filled with frictionless liquid, as a fundamental model before we proceed to the investigation of a container with both flexible side-wall and flexible bottom. Restricting the liquid–structure coupled system to such a model, a free vibration analysis has been conducted by many researchers [1–10], in which the flexible bottom was treated as an

0022-460X/02/140717 + 24 $35.00/0 © 2002 Elsevier Science Ltd.

elastic plate [2–4, 6–10] or as a membrane [1, 5, 7, 8]. In these studies, some are considering the effect of liquid surface tension [3–5, 7, 8] and determine its influence on the coupled sloshing natural frequencies. From these studies, in general, it has been found that coupled sloshing natural frequencies are generally reduced a little by the reduction of the bottom stiffness, while the effect of free surface tension increases the coupled sloshing natural frequencies. In such a system, the dynamic behavior of a liquid and a flexible bottom are coupled, the degree of which depends on the system parameters, i.e., liquid height, mass density ratio, stiffness of the bottom structure, etc. These conclusions are for systems which have a flexible bottom with relatively high rigidity, in which coupled sloshing natural frequencies and coupled bulging (bottom) natural frequencies are far apart from each other.

In the present study, assuming the bottom as a membrane and taking the effect of liquid free surface tension, we would like to treat the same model which has a stronger coupling, i.e., where the coupled sloshing and coupled bulging natural frequencies are of the same order, stemming from a strong reduction of the bottom flexibility or a strong effect of the liquid surface tension. Furthermore, by adding the usual free surface edge condition, i.e., the free surface moves up and down along the side-wall which is referred to as "slip" edge condition, we will consider another edge condition, i.e., the "anchored" edge condition in which the free surface exhibits a fixed contact line [11].

In the numerical calculations, at first, uncoupled vibration characteristics of a liquid in a rigid container for two edge conditions and membrane alone are presented. Then, the coupled vibration characteristics are investigated for different system parameters. And in the axisymmetric vibration mode with the anchored edge condition, appearance of a sloshing vibration mode which does not exist in a rigid bottom container was clarified, where a mode disappearance of the bottom due to the reduction of bottom stiffness was found.

It is to be added that some related studies have been conducted by Amabili *et al.* considering the effect of side-wall flexibility and ring-stiffeners of a container [12]. In addition, Chiba conducted a non-linear analysis [13, 14] and a response analysis of a liquid free surface with a flexible bottom motion [15].

2. BASIC EQUATIONS

A cylindrical container with a rigid side-wall and a membrane bottom is filled to height h with incompressible and inviscid liquid. We shall consider small amplitude coupled free vibrations of a liquid and a membrane bottom. Cylindrical co-ordinates are taken as shown in Figure 1. For small liquid velocities and small membrane deformation, the governing equations may be linearized. In addition, a static deformation of the membrane bottom is neglected. With the liquid motion assumed to be irrotational, the governing equation for the liquid velocity potential $\Phi(r, \theta, z, t)$ results in the Laplace equation

$$\nabla^2\Phi = 0, \qquad 0 < r < a, \qquad 0 < z < h,$$

$$\nabla^2 \equiv \frac{\partial^2}{\partial r^2} + \frac{1}{r}\frac{\partial}{\partial r} + \frac{1}{r^2}\frac{\partial^2}{\partial \theta^2} + \frac{\partial^2}{\partial z^2}, \tag{1}$$

which has to be solved with the appropriate boundary conditions.

With the free liquid surface displacement as $\Gamma(r, \theta, t)$, the boundary conditions at the free surface are the dynamic condition

$$\frac{\partial \Phi}{\partial t} + g\Gamma - \frac{\sigma}{\rho_f}\left[\frac{\partial^2 \Gamma}{\partial r^2} + \frac{1}{r}\frac{\partial \Gamma}{\partial r} + \frac{1}{r^2}\frac{\partial^2 \Gamma}{\partial \theta^2}\right] = const. \quad \text{at } z = h \tag{2}$$

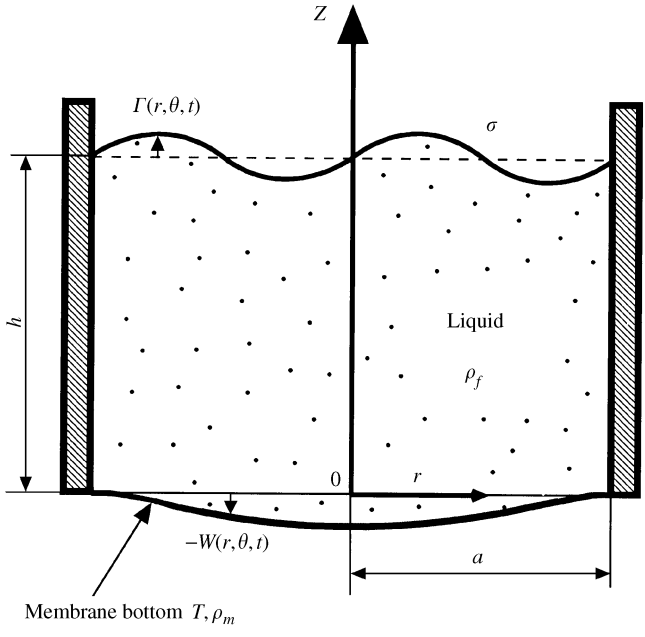

Figure 1. Cylindrical container with a membrane bottom filled with frictionless liquid.

and the kinematic condition

$$\frac{\partial \Phi}{\partial z} = \frac{\partial \Gamma}{\partial t} \text{ at } z = h, \tag{3}$$

where is g the gravitational acceleration, ρ_f the density and σ is the surface tension of the liquid. At the side-wall, the rigid wall condition is given by

$$\frac{\partial \Phi}{\partial r} = 0 \text{ at } 0 \leqslant z \leqslant h, \quad r = a. \tag{4}$$

At the bottom interface, the compatibility condition

$$\frac{\partial W}{\partial t} = \frac{\partial \Phi}{\partial z} \text{ at } z = 0 \tag{5}$$

has to be satisfied, so that the velocity of the membrane is equal to that of liquid at the bottom interface. With the displacement of the membrane bottom as $W(r, \theta, t)$, the equation of motion of the membrane is given as

$$T\left[\frac{\partial^2 W}{\partial r^2} + \frac{1}{r}\frac{\partial W}{\partial r} + \frac{1}{r^2}\frac{\partial^2 W}{\partial \theta^2}\right] = \rho_m \frac{\partial^2 W}{\partial t^2} - \rho_f \left.\frac{\partial \Phi}{\partial t}\right|_{z=0} - \rho_f g W \text{ at } z = 0 \tag{6}$$

and at the circumferential boundary of the bottom,

$$W = 0 \text{ at } r = a, \tag{7}$$

where T is the membrane tension and ρ_m is the mass per unit area of the membrane.

In order to get general results, it is convenient to use non-dimensional forms of the above equations as

$$\bar{\nabla}^2\phi = 0; \bar{\nabla}^2 = \frac{\partial^2}{\partial\rho^2} + \frac{\partial}{\rho\partial\rho} + \frac{1}{\rho^2}\frac{\partial^2}{\partial\theta^2} + \frac{\partial^2}{\partial\xi^2}, \tag{1'}$$

$$\frac{\partial\phi}{\partial\tau} + \frac{1}{c}\varsigma - \frac{\bar{\sigma}}{c}\left[\frac{\partial^2\varsigma}{\partial\rho^2} + \frac{1}{\rho}\frac{\partial\varsigma}{\partial\rho} + \frac{1}{\rho^2}\frac{\partial^2\varsigma}{\partial\theta^2}\right] = const. \text{ at } \xi = \ell_0, \tag{2'}$$

$$\frac{\partial\phi}{\partial\xi} = \frac{\partial\varsigma}{\partial\tau} \text{ at } \xi = \ell_0, \tag{3'}$$

$$\phi_{,\rho} = 0 \text{ at } \rho = 1, \tag{4'}$$

$$w_{,\tau} = \phi_{,\xi} \text{ at } \xi = 0, \tag{5'}$$

$$\left(\frac{\partial^2 w}{\partial\rho^2} + \frac{1}{\rho}\frac{\partial w}{\partial\rho} + \frac{1}{\rho^2}\frac{\partial^2 w}{\partial\vartheta^2}\right) = \frac{c}{\bar{T}}w_{,\tau\tau} - \frac{\bar{\rho}c}{\bar{T}}\phi_{,\tau} - \frac{\bar{\rho}}{\bar{T}}w \text{ at } \xi = 0, \tag{6'}$$

$$w = 0 \text{ at } \rho = 1, \tag{7'}$$

where the dimensionless values

$$\xi = \frac{z}{a}, \quad \rho = \frac{r}{a}, \quad w = \frac{W}{a}, \quad \phi = \frac{\Phi}{\Omega_0 a^2}, \quad \varsigma = \frac{\Gamma}{a}, \quad \tau = \Omega_0 t, \quad \Omega_0^2 = \frac{gc}{a}, \quad c = \varepsilon_{11}\tanh(\varepsilon_{11}),$$

$$l_0 = \frac{h}{a}, \quad \omega = \frac{\Omega}{\Omega_0}, \quad \bar{\sigma} = \frac{\sigma}{\rho_f a^2 g}, \quad \bar{\rho} = \frac{a\rho_f}{\rho_m}, \quad \bar{T} = \frac{T}{ag\rho_m}. \tag{8}$$

In the above equations, $\varepsilon_{11}(= 1{\cdot}84118)$ is a value which satisfies $J_1'(\varepsilon_{11}) = 0$, and Ω_0 is the first sloshing natural circular frequency in a rigid cylindrical tank with $m = 1$ and liquid height ratio $\ell_0 = 1{\cdot}0$. Then, the present coupled natural frequencies are normalized with this frequency.

3. METHOD OF SOLUTION

We consider here two free surface edge conditions. One is the slipping edge condition in which the free surface displacement moves up and down at the side-wall of the container, and the second is the anchored edge condition in which the free surface does not move at the circumferential edge [11], which may occur when a cylindrical container has rims with sharp edge. When the free liquid surface is located at such a sharp edge, its movement may be constrained. In addition, this is true when the liquid exhibits a strong surface tension. Both effects would require a treatment of the contact line of the free surface as an anchored edge.

The solution of the Laplace equation (1′) which satisfies rigid side-wall condition (4′), $\phi(\rho, \theta, \xi, \tau)$, free surface displacement $\varsigma(\rho, \theta, \tau)$ and membrane displacement $w(\rho, \theta, \tau)$ are assumed as

$$\phi(\rho, \theta, \xi, \tau) = \mathrm{i}\omega\mathrm{e}^{\mathrm{i}\omega\tau}\left[\phi_0(\rho, \xi) + \sum_{m=1}\phi_m(\rho, \theta, \xi)\right], \tag{9}$$

$$\phi_0(\rho, \xi) = A_0\xi + B_0 + \sum_n \mathrm{J}_0(\varepsilon_{0n}\rho)\left\{\frac{\sinh(\varepsilon_{0n}\xi)}{\cosh(\varepsilon_{0n}l_0)}A_{0n} + \frac{\cosh(\varepsilon_{0n}\xi)}{\sinh(\varepsilon_{0n}\ell_0)}B_{0n}\right\}, \tag{10}$$

$$\phi_m(\rho, \theta, \xi) = \sum_n \mathrm{J}_m(\varepsilon_{mn}\rho)\left\{\frac{\sinh(\varepsilon_{mn}\xi)}{\cosh(\varepsilon_{mn}l_0)}A_{mn} + \frac{\cosh(\varepsilon_{mn}\xi)}{\sinh(\varepsilon_{mn}\ell_0)}B_{mn}\right\}\cos m\theta, \tag{11}$$

$$\varsigma(\rho, \theta, \tau) = \mathrm{e}^{\mathrm{i}\omega\tau}\,\bar{\varsigma}(\rho, \theta), \tag{12}$$

$$\bar{\varsigma}(\rho, \theta) = \sum_{m=0}\sum_{n=1}\{f_0 + \varsigma_{mn}\mathrm{J}_m(\varepsilon_{mn}\rho)\}\cos m\theta, \tag{13}$$

$$w(\rho, \theta, \tau) = \mathrm{e}^{\mathrm{i}\omega\tau}\sum_{m=0}\sum_n w_{mn}\mathrm{J}_m(\beta_{mn}\rho)\cos m\theta, \tag{14}$$

where $\mathrm{J}_m(\ )$ is the mth order Bessel functions of the first kind, A_0, B_0, A_{0n}, B_{0n}, A_{mn}, B_{mn}, ς_{mn}, w_{mn} are unknown coefficients, while ε_{0n}, ε_{mn}, β_{mn} are the parameters which satisfy $\mathrm{J}'_0(\varepsilon_{0n}) = 0$, $\mathrm{J}'_m(\varepsilon_{mn}) = 0$, $\mathrm{J}_m(\beta_{mn}) = 0$ respectively. ω is the natural circular frequency.

3.1. SLIPPING EDGE CONDITION

In this case, the liquid free surface conditions, represented by two equations (2′) and (3′), can be combined into one equation as

$$\phi_{,\tau\tau} + \frac{\bar{\sigma}}{c}\phi_{,\xi\xi\xi} + \frac{1}{c}\phi_{,\xi} = 0 \text{ at } \xi = l_0. \tag{15}$$

3.1.1. *Asymmetric vibration* ($m \neq 0$)

From the compatibility condition (5′) at the bottom, A_{mn} can be represented in terms of w_{mk} as

$$A_{mn} = \frac{-2\cosh(\varepsilon_{mn}l_0)}{\varepsilon_{mn}[1 - (m/\varepsilon_{mn})^2]\mathrm{J}_m(\varepsilon_{mn})}\sum_k \frac{\beta_{mk}\mathrm{J}'_m(\beta_{mk})}{(\beta_{mk}^2 - \varepsilon_{mn}^2)}w_{mk}. \tag{16}$$

The liquid free surface condition (15) is represented as

$$\frac{1}{c}(\bar{\sigma}\varepsilon_{mn}^3 + \varepsilon_{mn})(A_{mn} + B_{mn}) - \omega^2\{\tanh(\varepsilon_{mn}l_0)A_{mn} + \coth(\varepsilon_{mn}l_0)B_{mn}\} = 0. \tag{17}$$

The equation of motion of the membrane (6′) renders as

$$L_m(w) = \sum_n w_{mn}\left(\frac{\bar{\rho}}{\bar{T}} - \beta_{mn}^2\right)\mathrm{J}_m(\beta_{mn}\rho) - \frac{c}{\bar{T}}\omega^2\left\{\bar{\rho}\sum_n \frac{\mathrm{J}_{mn}(\varepsilon_{mn}\rho)}{\sinh(\varepsilon_{mn}l_0)}B_{mn} - \mathrm{J}_m(\beta_{mn}\rho)w_{mn}\right\}. \tag{18}$$

Applying the Galerkin method

$$\int_0^{2\pi}\int_0^1 L_m(w)\mathrm{J}_m(\beta_{mp}\rho)\cos q\theta\ \rho\,\mathrm{d}\rho\,\mathrm{d}\theta, \qquad p = 1, 2, \ldots, n, \tag{19}$$

yields

$$\frac{\mathrm{J}'_m(\beta_{mp})}{c}\left(1-\frac{\bar{T}}{\bar{\rho}}\,\beta_{mp}^2\right)w_{mp}-\omega^2\left[2\sum_n\frac{\beta_{mp}\mathrm{J}_m(\varepsilon_{mn})B_{mn}}{(\beta_{mp}^2-\varepsilon_{mn}^2)\sinh(\varepsilon_{mn}l_0)}-\frac{J'_m(\beta_{mp})}{\bar{\rho}}\,w_{mp}\right]=0,$$

$$p=1,2,\ldots,k. \tag{20}$$

Introducing equation (16) into equation (17), equations (17) and (20) represent the $(n+k)$ coupled linear algebraic equations in terms of B_{mn} and w_{mk}, and they are represented in a matrix form as equation (21). Then, the problem is reduced to the eigenvalue problem from which one can get coupled natural frequencies as an eigenvalue, which is

$$\left[\begin{pmatrix}\frac{1}{c}(\bar{\sigma}\varepsilon_{ms}^3+\varepsilon_{ms})\delta_{ns} & -\frac{2(\bar{\sigma}\varepsilon_{ms}^3+\varepsilon_{ms})\cosh(\varepsilon_{ms}l_0)}{c\varepsilon_{ms}[1-(m/\varepsilon_{ms})^2]\mathrm{J}_m(\varepsilon_{ms})}\frac{\beta_{mk}\mathrm{J}'_m(\beta_{mk})}{(\beta_{mk}^2-\varepsilon_{ms}^2)}\\ 0 & \frac{\mathrm{J}'_m(\beta_{mr})}{c}\left\{1-\frac{\bar{T}}{\bar{\rho}}\beta_{mr}^2\right\}\delta_{rk}\end{pmatrix}\right.$$

$$\left.-\omega^2\begin{pmatrix}\coth(\varepsilon_{ms}l_0)\,\delta_{ns} & -\frac{2\sinh(\varepsilon_{ms}l_0)}{\varepsilon_{ms}[1-(m/\varepsilon_{ms})^2]\mathrm{J}_m(\varepsilon_{ms})}\frac{\beta_{mk}\mathrm{J}'_m(\beta_{mk})}{(\beta_{mk}^2-\varepsilon_{ms}^2)}\\ \frac{2\beta_{mr}\mathrm{J}_m(\varepsilon_{mn})}{(\beta_{mr}^2-\varepsilon_{mn}^2)\sinh(\varepsilon_{mn}l_0)} & -\frac{1}{\bar{\rho}}\,\mathrm{J}'_m(\beta_{mr})\,\delta_{rk}\end{pmatrix}\right]\begin{Bmatrix}B_{mn}\\ w_{mk}\end{Bmatrix}=\{0\},$$

$$s=1,\ldots,n;\ r=1,\ldots,k. \tag{21}$$

3.1.2. *Axisymmetric vibration* ($m=0$)

With a similar procedure in the asymmetric vibration, A_0 and A_{0n} are represented in terms of w_{0k} as

$$A_0=2\sum_k\frac{\mathrm{J}_1(B_{0k})}{\beta_{0k}}\,w_{0k}, \tag{22}$$

$$A_{0n}=\frac{2\cosh(\varepsilon_{0n}l_0)}{\varepsilon_{0n}\mathrm{J}_0(\varepsilon_{0n})}\sum_k\frac{\mathrm{J}_1(\beta_{0k})\beta_{0k}}{(\beta_{0k}^2-\varepsilon_{0n}^2)}\,w_{0k}. \tag{23}$$

The liquid free surface condition (15) yields

$$\frac{A_0}{c}-\omega^2\,(l_0A_0+B_0)=0, \tag{24}$$

$$\frac{1}{c}(\bar{\sigma}\varepsilon_{0n}^3+\varepsilon_{0n})(A_{0n}+B_{0n})-\omega^2\{\tanh(\varepsilon_{0n}l_0)A_{0n}+\coth(\varepsilon_{0n}l_0)B_{0n}\}=0. \tag{25}$$

From the equation of motion of the membrane (6′) we obtain

$$\frac{\mathrm{J}_1(\beta_{0p})}{c}\left\{1-\frac{\bar{T}}{\bar{\rho}}\beta_{0p}^2\right\}w_{0p}-\omega^2\left[2\left\{\frac{B_0}{\beta_{0p}}+\beta_{0p}\sum_n\frac{\mathrm{J}_0(\varepsilon_{0n})B_{0n}}{(\beta_{0p}^2-\varepsilon_{0n}^2)\sinh(\varepsilon_{0n}l_0)}\right\}-\frac{\mathrm{J}_1(\beta_{0p})}{\bar{\rho}}w_{0p}\right]=0,$$

$$p=1,2,\ldots,k. \tag{26}$$

Finally, we obtain $(1+n+k)$ coupled linear algebraic equations (27) in terms of B_0, B_{0n} and w_{0k}.

It is therefore

$$\left[\begin{pmatrix} 0 & 0 & \dfrac{2}{c}\dfrac{\mathrm{J}_1(\beta_{0k})}{\beta_{0k}} \\ 0 & \dfrac{1}{c}(\bar{\sigma}\varepsilon_{os}^3 + \varepsilon_{os})\,\delta_{ns} & \dfrac{2(1+\bar{\sigma}\varepsilon_{0s}^2)\cosh(\varepsilon_{0s}l_0)}{c\mathrm{J}_0(\varepsilon_{0s})}\dfrac{\mathrm{J}_1(\beta_{0k})\beta_{0k}}{(\beta_{0k}^2 - \varepsilon_{0s}^2)} \\ 0 & 0 & \dfrac{\mathrm{J}_1(\beta_{0r})}{c}\left\{1 - \dfrac{\bar{T}}{\bar{\rho}}\beta_{0r}^2\right\}\delta_{rk} \end{pmatrix}\right.$$

$$\left. - \omega^2\begin{pmatrix} 1 & 0 & 2l_0\dfrac{\mathrm{J}_1(\beta_{0k})}{\beta_{0k}} \\ 0 & \coth(\varepsilon_{0s}l_0) & \dfrac{2\sinh(\varepsilon_{0s}l_0)}{\varepsilon_{0s}\mathrm{J}_0(\varepsilon_{0s})}\dfrac{\mathrm{J}_1(\beta_{0k})\beta_{0k}}{(\beta_{0k}^2 - \varepsilon_{0s}^2)} \\ \dfrac{2}{\beta_{0r}} & \dfrac{2\beta_{0r}\mathrm{J}_0(\varepsilon_{0n})}{(\beta_{0r}^2 - \varepsilon_{0n}^2)\sinh(\varepsilon_{0n}l_0)} & -\dfrac{\mathrm{J}_1(\beta_{0r})}{\bar{\rho}}\delta_{rk} \end{pmatrix}\right]\begin{Bmatrix} B_0 \\ B_{0n} \\ w_{0sk} \end{Bmatrix} = \{0\},$$

$$s = 1, \ldots, n;\ r = 1, \ldots, k. \quad (27)$$

3.2. ANCHORED EDGE CONDITION

In this case, the liquid free surface displacement is zero at the wall, i.e.,

$$\varsigma(1, \theta, \tau) = 0 \text{ at } \rho = 1. \quad (28)$$

3.2.1. *Asymmetric vibration* ($m \neq 0$)

Introducing equation (12) into the dynamic liquid free surface condition (2′) yields

$$\frac{\mathrm{d}^2\bar{\varsigma}}{\mathrm{d}\rho^2} + \frac{1}{\rho}\frac{\mathrm{d}\bar{\varsigma}}{\mathrm{d}\rho} - \frac{1}{\bar{\sigma}}\bar{\varsigma} = -\omega^2\frac{c}{\bar{\sigma}}\sum_n \mathrm{J}_m(\varepsilon_{mn}\rho)\{\tanh(\varepsilon_{mn}\ell_0)A_{mn} + \coth(\varepsilon_{mn}\ell_0)B_{mn}\}, \quad (29)$$

which gives the solution

$$\bar{\varsigma}(\rho) = C_m\mathrm{I}_m(\beta\rho) + \omega^2\frac{c}{\bar{\sigma}}\sum_n \frac{\mathrm{J}_m(\varepsilon_{mn}\rho)}{(\varepsilon_{mn}^2 + \beta^2)}\{\tanh(\varepsilon_{mn}\ell_0)A_{mn} + \coth(\varepsilon_{mn}\ell_0)B_{mn}\}, \quad (30)$$

where $\beta^2 \equiv 1/\bar{\sigma}$.

The anchored edge condition (28) renders

$$C_m\mathrm{I}_m(\beta) + \omega^2\frac{c}{\bar{\sigma}}\sum_n \frac{\mathrm{J}_m(\varepsilon_{mn})}{(\varepsilon_{mn}^2 + \beta^2)}\{\tanh(\varepsilon_{mn}\ell_0)A_{mn} + \coth(\varepsilon_{mn}\ell_0)B_{mn}\} = 0. \quad (31)$$

While the kinematic liquid free surface condition (3′) yields by means of Bessel–Fourier series equation of $\mathrm{I}_m(\beta\rho)$

$$\mathrm{I}_m(\beta\rho) = 2\beta\sum_{n=1}^{\infty}\frac{\varepsilon_{mn}^2\mathrm{I}'_m(\beta)\mathrm{J}_m(\varepsilon_{mn}\rho)}{\mathrm{J}_m(\varepsilon_{mn})(\varepsilon_{mn}^2 + \beta^2)(\varepsilon_{mn}^2 - m^2)}, \quad (32)$$

the expression

$$\frac{2\beta \mathrm{I}'_m(\beta)\varepsilon_{mn}^2}{\mathrm{J}_m(\varepsilon_{mn})(\varepsilon_{mn}^2 - m^2)} C_m - \varepsilon_{mn}(\varepsilon_{mn}^2 + \beta^2)(A_{mn} + B_{mn}) + \omega^2 \frac{c}{\bar{\sigma}} \{\tanh(\varepsilon_{mn}\ell_0) A_{mn} + \coth(\varepsilon_{mn}\ell_0) B_{mn}\} = 0. \tag{33}$$

Using equation (31), C_m in equation (33) can be eliminated, and introducing equation (16), A_{mn} can be represented in terms of w_{mk}, and finally we obtain

$$\begin{aligned}
&\frac{1}{c}(1 + \bar{\sigma}\varepsilon_{ms}^2) \left\{ \varepsilon_{ms} B_{ms} - \frac{2\cosh(\varepsilon_{ms}\ell_0)}{\mathrm{J}_m(\beta_{ms})[1 - (m/\varepsilon_{ms})^2]} \sum_k \frac{\beta_{mk} \mathrm{J}'_m(\beta_{mk})}{(\beta_{mk}^2 - \varepsilon_{ms}^2)} w_{mk} \right\} \\
&\quad - \omega^2 \left[\coth(\varepsilon_{ms}\ell_0) B_{ms} - \frac{2\beta \mathrm{I}'_m(\beta)}{\mathrm{I}_m(\beta)\mathrm{J}_m(\varepsilon_{ms})[1 - (m/\varepsilon_{ms})^2]} \sum_n \frac{\mathrm{J}_m(\varepsilon_{mn})}{(\varepsilon_{mn}^2 + \beta^2)} \coth(\varepsilon_{mn}\ell_0) B_{mn} \right. \\
&\quad - \frac{2}{\varepsilon_{ms}\mathrm{J}_m(\varepsilon_{mr})[1 - (m/\varepsilon_{ms})^2]} \sum_k \beta_{mk} \mathrm{J}'_m(\beta_{mk}) \left\{ \frac{\sinh(\varepsilon_{ms}\ell_0)}{(\beta_{mk}^2 - \varepsilon_{ms}^2)} - \frac{2\beta I'_m(\beta)\varepsilon_{ms}}{\mathrm{I}_m(\beta)} \right. \\
&\quad \left. \left. \times \sum_j \frac{\varepsilon_{mj} \sinh(\varepsilon_{mj}\ell_0)}{(\varepsilon_{mj}^2 + \beta^2)(\varepsilon_{mj}^2 - m^2)(\beta_{mk}^2 - \varepsilon_{mj}^2)} \right\} w_{mk} \right] = 0,
\end{aligned} \tag{34}$$

which is the kinematic liquid free surface condition satisfying the edge anchored condition.

The membrane equation is the same as the slipping case, i.e., equation (20). Equations (34) and (20) represent the $(n + k)$ coupled linear algebraic equations in terms of B_{mn} and w_{mk}.

3.2.2. *Axisymmetric vibration* ($m = 0$)

In this case, from the kinematic condition of the free surface we obtain

$$f_0 = A_0, \qquad \varsigma_{0n} = \varepsilon_{0n}(A_{0n} + B_{0n}). \tag{35, 36}$$

With a similar procedure as in the asymmetric case, we finally obtain coupled equations in terms of B_0, B_{0n}, w_{0k}. Details of those equations are omitted here due to limited space.

4. NUMERICAL RESULTS

Some of the analytical results obtained above have been evaluated numerically. For reasons of space, we have concentrated only on the results for asymmetric vibration ($m = 1$) and axisymmetric vibration ($m = 0$) with both slipping and anchored free surface edge conditions. Their first radial modes n are, due to the large slosh masses participating in the motion, of great practical importance. For this reason, we focus on the lowest four coupled sloshing and bulging modes in which the liquid free surface and the membrane bottom motions are predominant respectively. The unknown parameters used in the calculation, i.e., n and k in equation (21), were used for four terms for both liquid and membrane parameters.

The present liquid–membrane coupled system is represented for the system parameters: membrane tension parameter $\bar{T} \equiv T/ag\rho_m$, liquid surface tension parameter $\bar{\sigma} \equiv \sigma/a^2 g\rho_f \equiv 1/Bo$, mass ratio parameter $\bar{\rho} \equiv a\rho_f/\rho_m$, liquid height ratio $\ell_0 \equiv h/a$, circumferential vibration mode number m, and radial vibration mode number n.

4.1. UNCOUPLED NATURAL FREQUENCIES

Before proceeding to investigate the liquid–membrane coupled dynamic system, we shall look at the uncoupled sloshing and membrane vibrational characteristics. Uncoupled sloshing natural frequencies $\omega_{mn}^{(\ell)}$ for a liquid of liquid height ℓ_0 in a container with rigid bottom and rigid wall, have been evaluated for the modes $m = 1$ and 0 when $\bar{\sigma} = 5{\cdot}0 \times 10^{-4}$ and 1·0. The results are shown in Figure 2. In this figure, thicker lines and thinner lines correspond to the results for the anchored and slipping edge conditions respectively. The lowest slipping natural sloshing frequency with $m = 1$ (in Figure 2(a)) tends to unity for very small surface tension $\bar{\sigma}$ with the increase of ℓ_0. This is due to the non-dimensionalization with parameter (c) in equation (8). This means that in the present study, calculated uncoupled and coupled frequencies are all normalized with the first sloshing natural frequency of a liquid with slipping edge conditions without surface tension of the asymmetric mode $m = 1$ when $\ell_0 = 1{\cdot}0$. Natural frequencies for the anchored case are a little higher than those of the slipping case, due to the constraint of the free surface displacement at the edge (Figure 2(a)). It may be noticed that the difference becomes prominent for a larger value of $\bar{\sigma}$(Figure 2(b)).

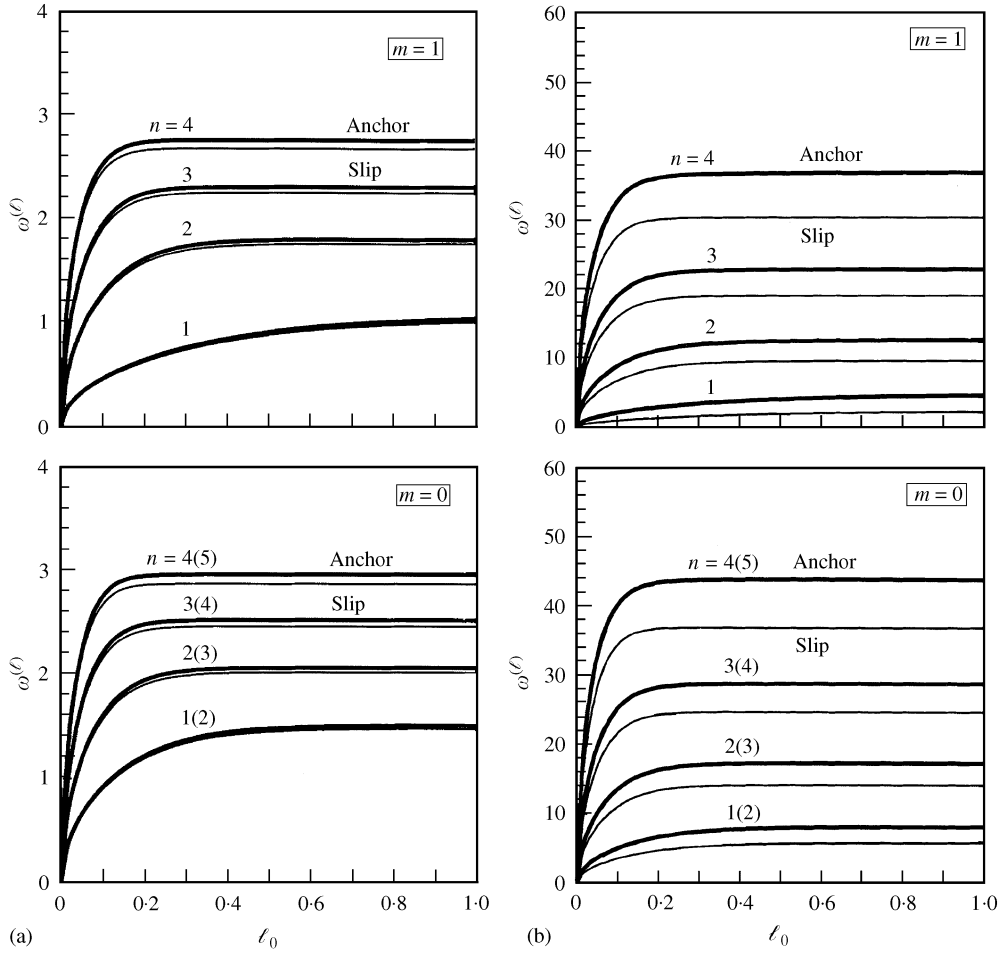

Figure 2. Uncoupled normalized sloshing natural frequency as a function of filling rate ℓ_0, $m = 1$, 0: ——, anchor; ——, slip. (a) $\bar{\sigma} = 5 \times 10^{-4}$, and (b) $\bar{\sigma} = 1{\cdot}0$.

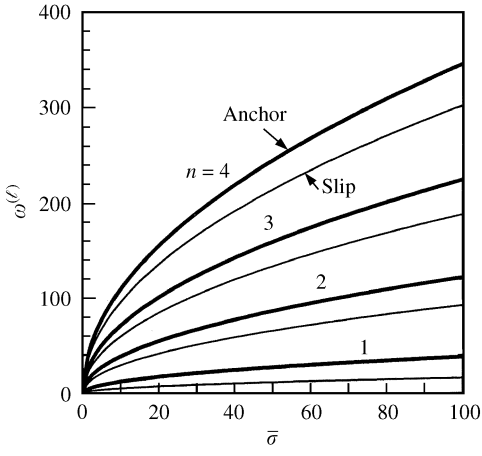

Figure 3. Uncoupled normalized sloshing natural frequency as a function of liquid surface tension $\bar{\sigma}$, $m = 1$, $\ell_0 = 0{\cdot}5$: ——, anchor; – – –, slip.

The influence of liquid surface tension $\bar{\sigma}$ on the uncoupled sloshing frequencies is presented in Figure 3, for the mode $m = 1$, when $\ell_0 = 0{\cdot}5$. In the case of slipping condition, the natural frequencies are simply given by

$$\omega_{mn}^{(l)} = \sqrt{\frac{\varepsilon_{mn}(1 + \varepsilon_{mn}^2 \bar{\sigma}) \tanh(\varepsilon_{mn} \ell_0)}{c}}. \tag{37}$$

From this equation, we find that the presence of the liquid free surface tension increases the natural frequency of the liquid. The vibration modes of a liquid free surface are displayed in Figure 4(a) for $m = 1$, and in Figure 4(b) for $m = 0$, for both slipping and anchored edge condition, respectively, and $\bar{\sigma} = 1{\cdot}0$, $\ell_0 = 0{\cdot}5$. In these figures, the maximum of the free surfaces are normalized to unity. It is to be noted that the lowest vibration mode for the axisymmetric vibration with anchored edge condition is $n = 2$ which has one nodal point in the radial direction, while the mode $n = 1$ cannot exist due to the volume conservation in a rigid container.

While uncoupled normalized membrane natural frequencies $\omega_{mn}^{(m)}$ are given by

$$\omega_{mn}^{(m)} = \beta_{mn} \sqrt{\frac{\bar{T}}{c}}, \tag{38}$$

which describes that the natural frequencies are proportional to the square root of $\bar{T}$. They are represented in Figure 5 for the modes $m = 0, 1, 2$ and $n = 1, 2, 3$. The values β_{mn} are the roots of the Bessel function $J_m(\beta) = 0$.

4.2. COUPLED VIBRATION BETWEEN LIQUID AND MEMBRANE

The coupled normalized natural frequencies of a liquid and a membrane bottom are considered by investigating the effects of $\bar{T}$, $\bar{\sigma}$ and $\bar{\rho}$. In Figure 6, the coupled natural frequency variations with liquid height ℓ_0 are represented for slipping edge condition for the asymmetric mode $m = 1$, $\bar{\rho} = 100$, $\bar{T} = 10^6$, when (a) $\bar{\sigma} = 1$, (b) $\bar{\sigma} = 10$, (c) $\bar{\sigma} = 100$. For reference, the uncoupled sloshing frequencies $\omega_{mn}^{(l)}$ are presented with dot–dashed lines. In

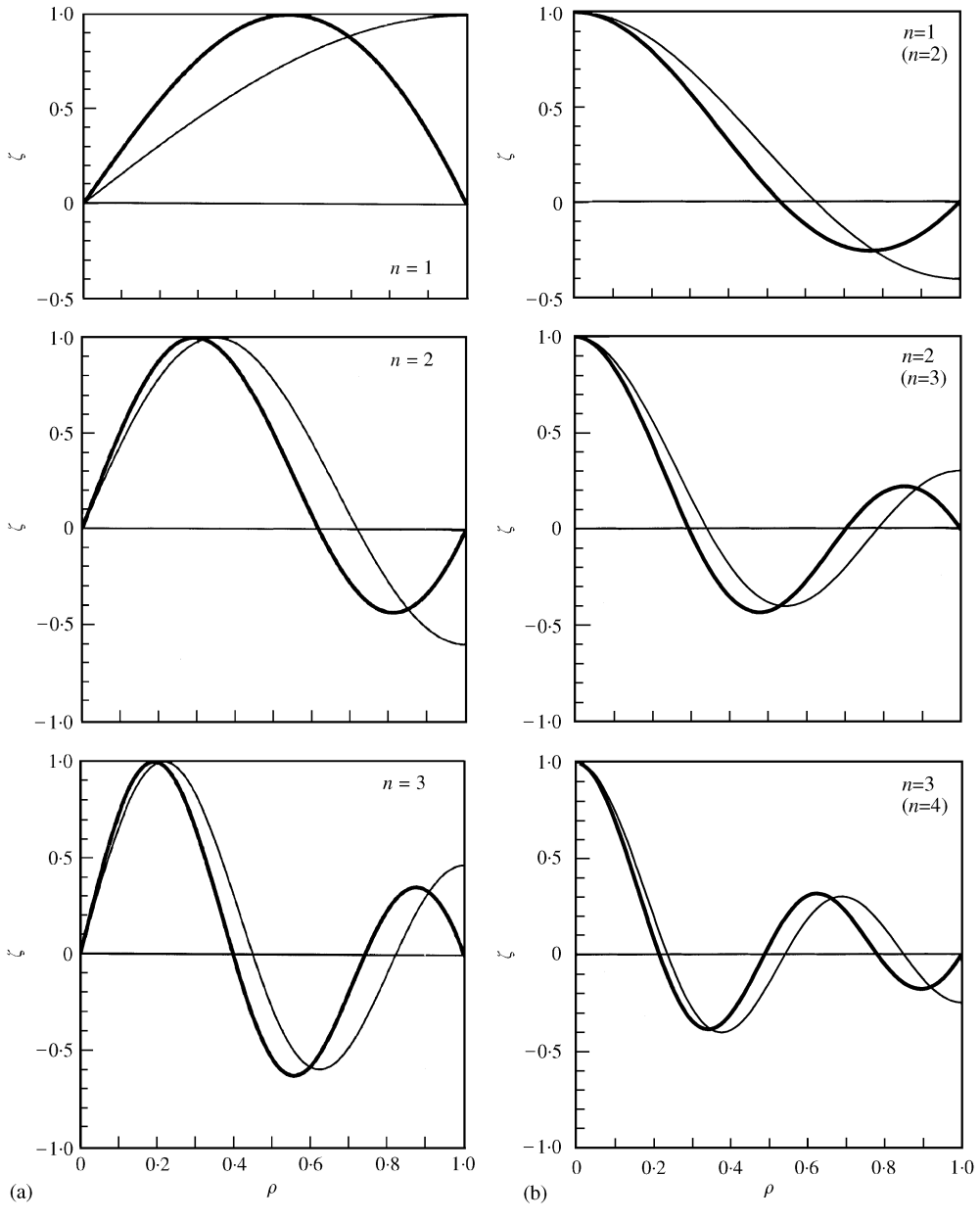

Figure 4. Uncoupled sloshing modes, $\bar{\sigma} = 1$, $\ell_0 = 0{\cdot}5$: ———, anchor; ——, slip. (a) $m = 1$, and (b) $m = 0$.

this figure, the lines of coupled and uncoupled results cannot be distinguished. As is shown, the coupled sloshing frequencies increase with increase of ℓ_0, while the coupled bulging (membrane) frequencies decrease due to the added mass effect of the liquid. Although the lowest four sloshing and four bulging (membrane) modes are calculated, we can recognize four sloshing modes and one bulging mode for $n = 1$ for the presented range of the figure. This is due to the larger difference between the coupled sloshing and the coupled membrane

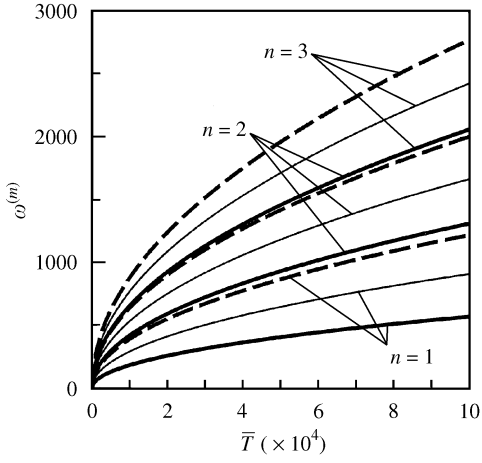

Figure 5. Uncoupled normalized membrane natural frequency $\omega^{(m)}$ as a function of tension $\bar{T}$: – – – –, $m = 0$; ——, $m = 1$; – – – –, $m = 2$.

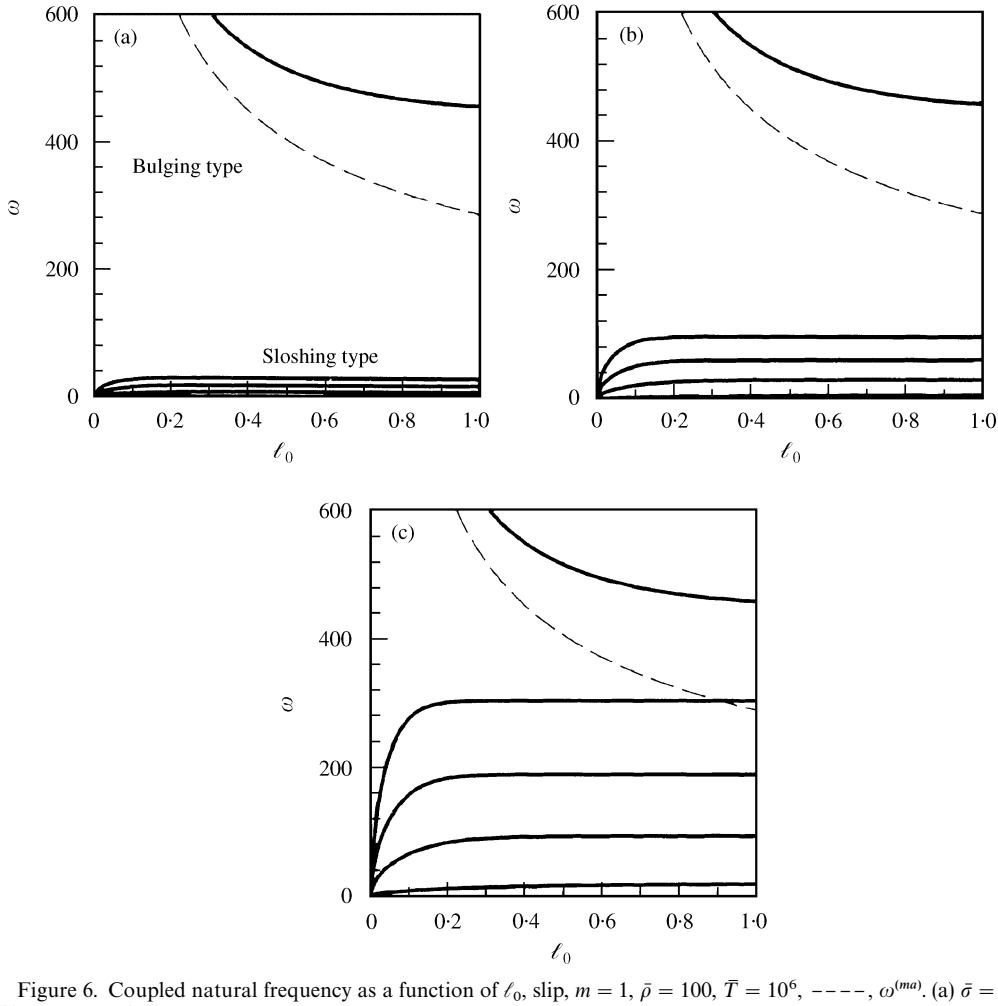

Figure 6. Coupled natural frequency as a function of ℓ_0, slip, $m = 1$, $\bar{\rho} = 100$, $\bar{T} = 10^6$, – – – –, $\omega^{(ma)}$. (a) $\bar{\sigma} = 1$, (b) $\bar{\sigma} = 10$, and (c) $\bar{\sigma} = 100$.

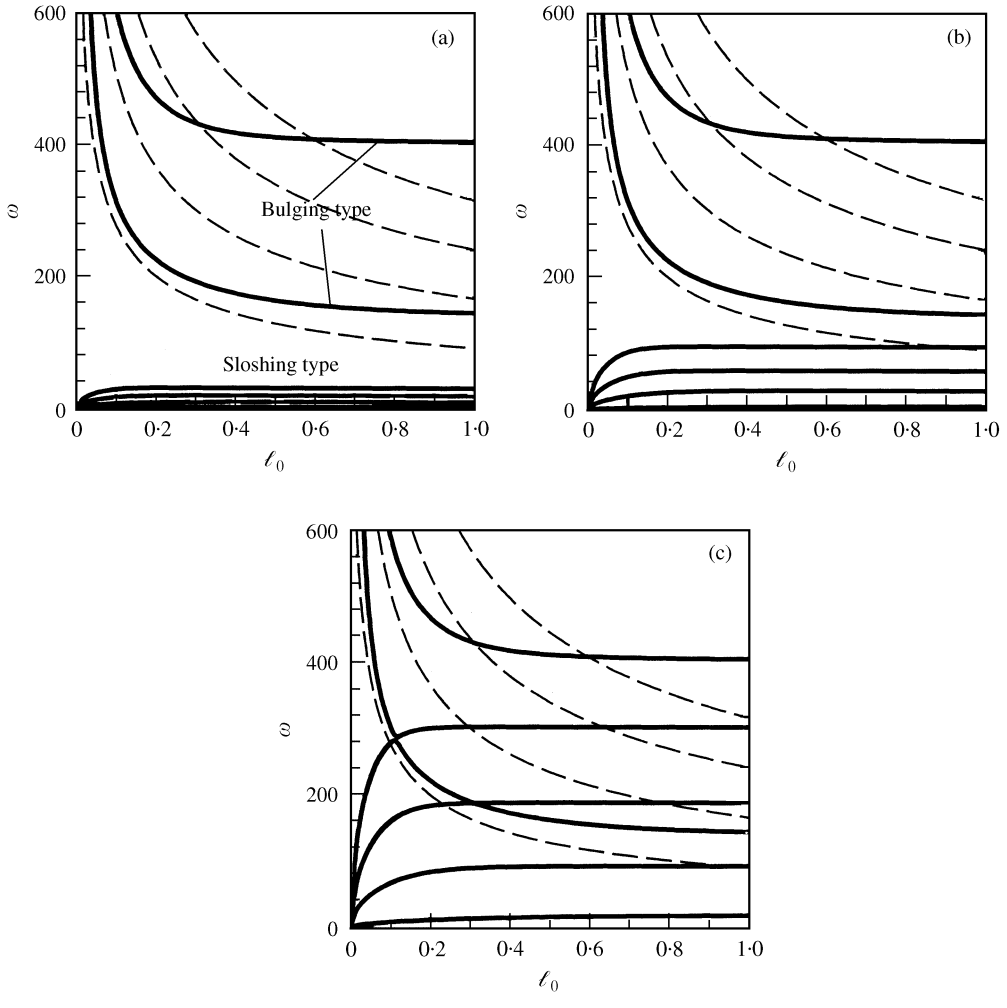

Figure 7. Coupled natural frequency as a function of ℓ_0, slip, $m = 1$, $\bar{\rho} = 100$, $\bar{T} = 10^5$, – – – –, $\omega^{(ma)}$. (a) $\bar{\sigma} = 1$, (b) $\bar{\sigma} = 10$, and (c) $\bar{\sigma} = 100$.

frequencies. These differences become smaller as $\bar{\sigma}$ increases to 10 and 100, as shown in Figure 6(b) and 6(c), indicating increased coupling effects.

Broken lines in the figure are frequencies of a membrane with added (non-sloshing) liquid mass, which are given by

$$\omega_{mn}^{(ma)} = \beta_{mn} \sqrt{\frac{\bar{T}}{c(1 + \bar{\rho}\ell_0)}}. \tag{39}$$

In the present case shown in Figure 6, $\omega_{11}^{(ma)}$ is lower than the coupled bulging frequency.

We notice that every time the sloshing and bulging frequencies approach each other, there will be a strong interaction and coupling between them. This will be expressed by the change of the coupled frequencies and their mode shapes. The magnitude of these changes shall, of course, depend on the magnitude of the generalized masses of the sloshing and the bulging. We expect for that reason that the interaction of the first sloshing mode with the

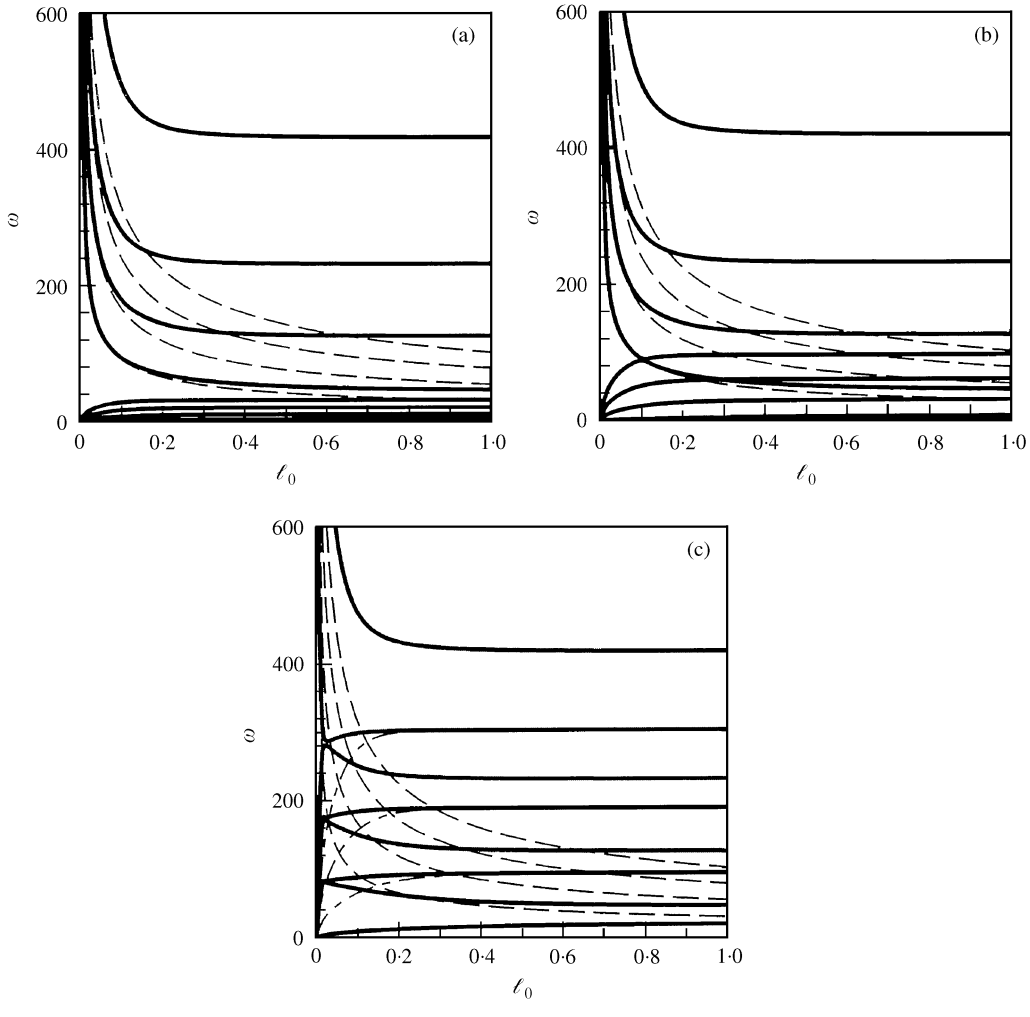

Figure 8. Coupled natural frequency as a function of ℓ_0, slip, $m = 1$, $\bar{\rho} = 1000$, $\bar{T} = 10^5$, – – – –, $\omega^{(ma)}$. (a) $\bar{\sigma} = 1$, (b) $\bar{\sigma} = 10$, and (c) $\bar{\sigma} = 100$.

first membrane mode will (due to their large generalized masses) present the most important interaction. Higher modes exhibit increasingly reduced generalized masses and shall for that reason, even for the coalescence of the natural frequencies, exhibit minor interaction effects.

When the membrane tension is reduced to $\bar{T} = 10^5$ (Figure 7), while keeping the other system parameters the same, the coupled bulging frequencies decrease and the sloshing and the bulging-type natural frequencies get close to each other, i.e., coupling becomes stronger, as shown in Figure 7(c). Strong dynamic coupling can be seen between the liquid and the membrane motions, where an order of exchange occurs between the vibration modes. Furthermore, $\omega_{11}^{(ma)}$ variations with ℓ_0 agree well with those of the coupled bulging frequency.

If the mass ratio is increased to $\bar{\rho} = 1000$, i.e., the liquid density becomes relatively large, as shown in Figure 8, the increase of the added liquid mass to the membrane decreases the bulging-type frequencies drastically with ℓ_0. This causes a strong coupling between the liquid and membrane motions. In Figure 9, similar results for the axisymmetric mode

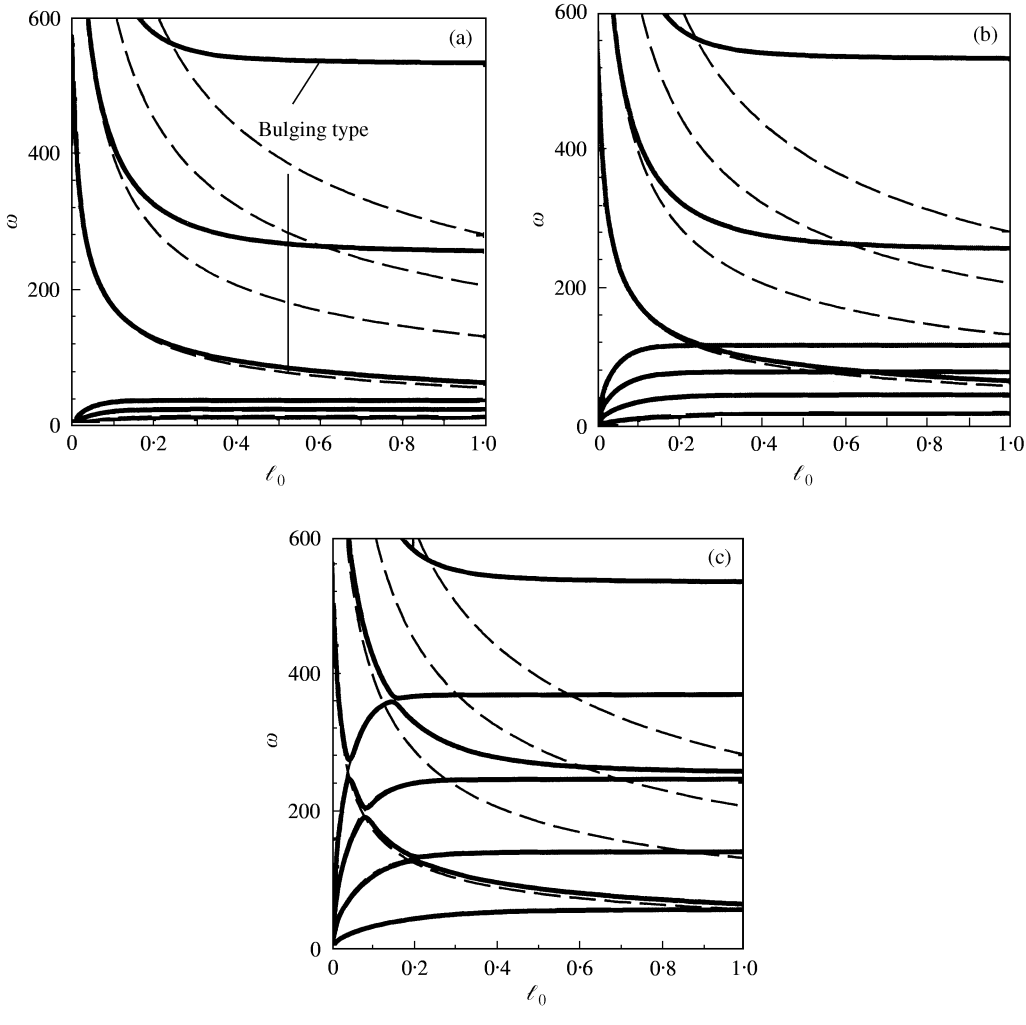

Figure 9. Coupled natural frequency as a function of ℓ_0, slip, $m = 0$, $\bar{\rho} = 100$, $\bar{T} = 10^5$, – – – –, $\omega^{(ma)}$. (a) $\bar{\sigma} = 1$, (b) $\bar{\sigma} = 10$, and (c) $\bar{\sigma} = 100$.

($m = 0$) are presented for the parameters as those of Figure 7 ($m = 1$). In this mode, the uncoupled frequencies of the membrane and the liquid are close to each other, and their coupling is for that reason stronger than those of the mode $m = 1$ (Figure 7). Furthermore, $\omega_{01}^{(ma)}$ variations with ℓ_0 agree well with those of the coupled bulging frequency.

To observe the influence of the free surface edge conditions, the results of anchored conditions for $m = 1$ and 0 are presented in Figure 10 by thicker lines. System parameters of these results are the same as those of the slipping case shown in Figures 7 and 9, where a smaller membrane tension $\bar{T} = 10^5$ has been employed. The slipping results are represented by thinner lines, for reference. As may be seen in the figure, the coupled bulging frequencies are nearly the same as those of the slipping edge conditions, while coupled sloshing frequencies are different as was already observed from the results of a rigid container (Figures 2 and 3).

So far, we have investigated the coupling between membrane bottom and liquid by viewing the coupled frequencies of the system. A better insight into the behavior of the

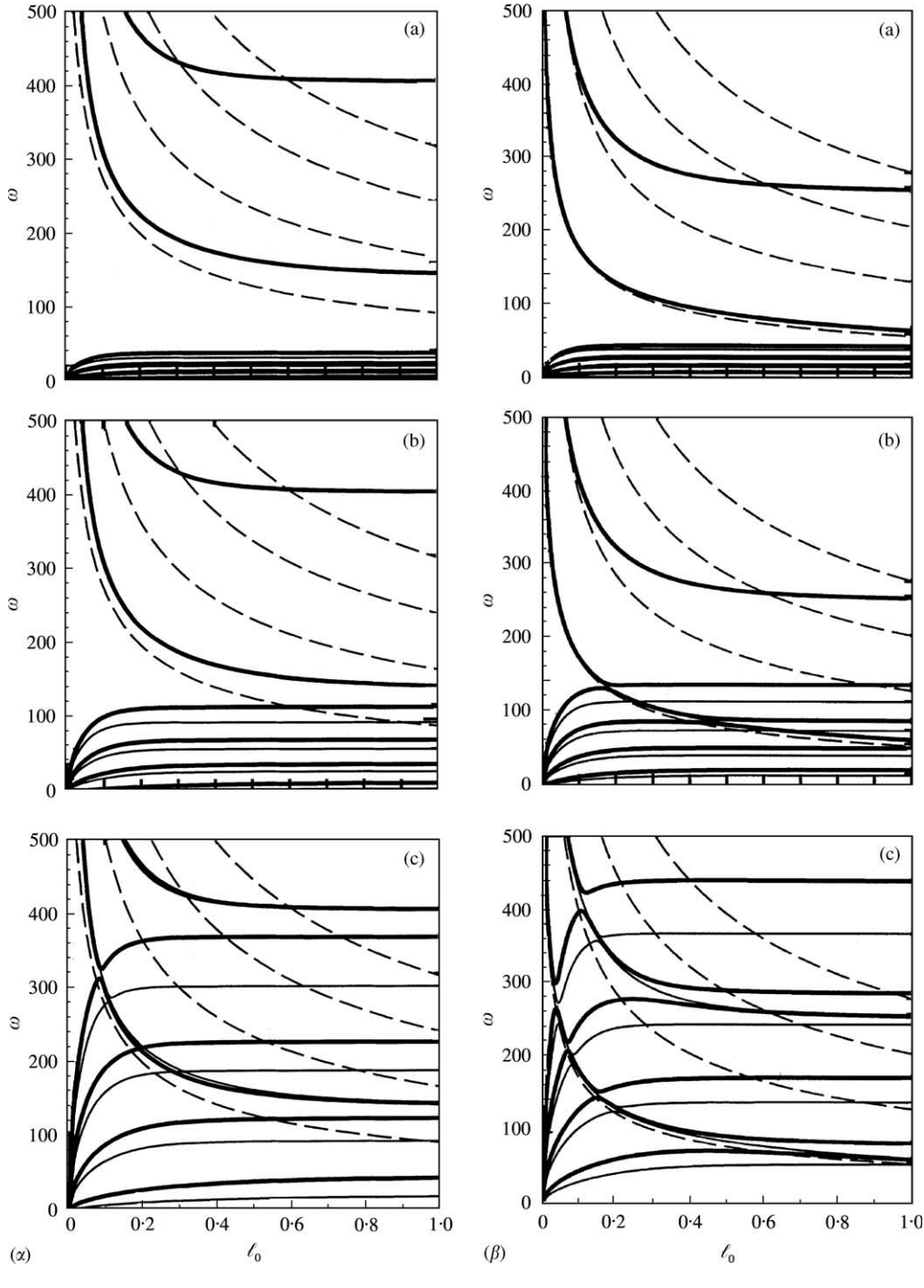

Figure 10. Coupled natural frequency as a function of ℓ_0: ——, anchor; ——, slip. $\bar{\rho} = 100$, $\bar{T} = 10^5$, – – – –, $\omega^{(ma)}$. (a) $\bar{\sigma} = 1$, (b) $\bar{\sigma} = 10$, (c) $\bar{\sigma} = 100$; (α) $m = 1$, (β) $m = 0$.

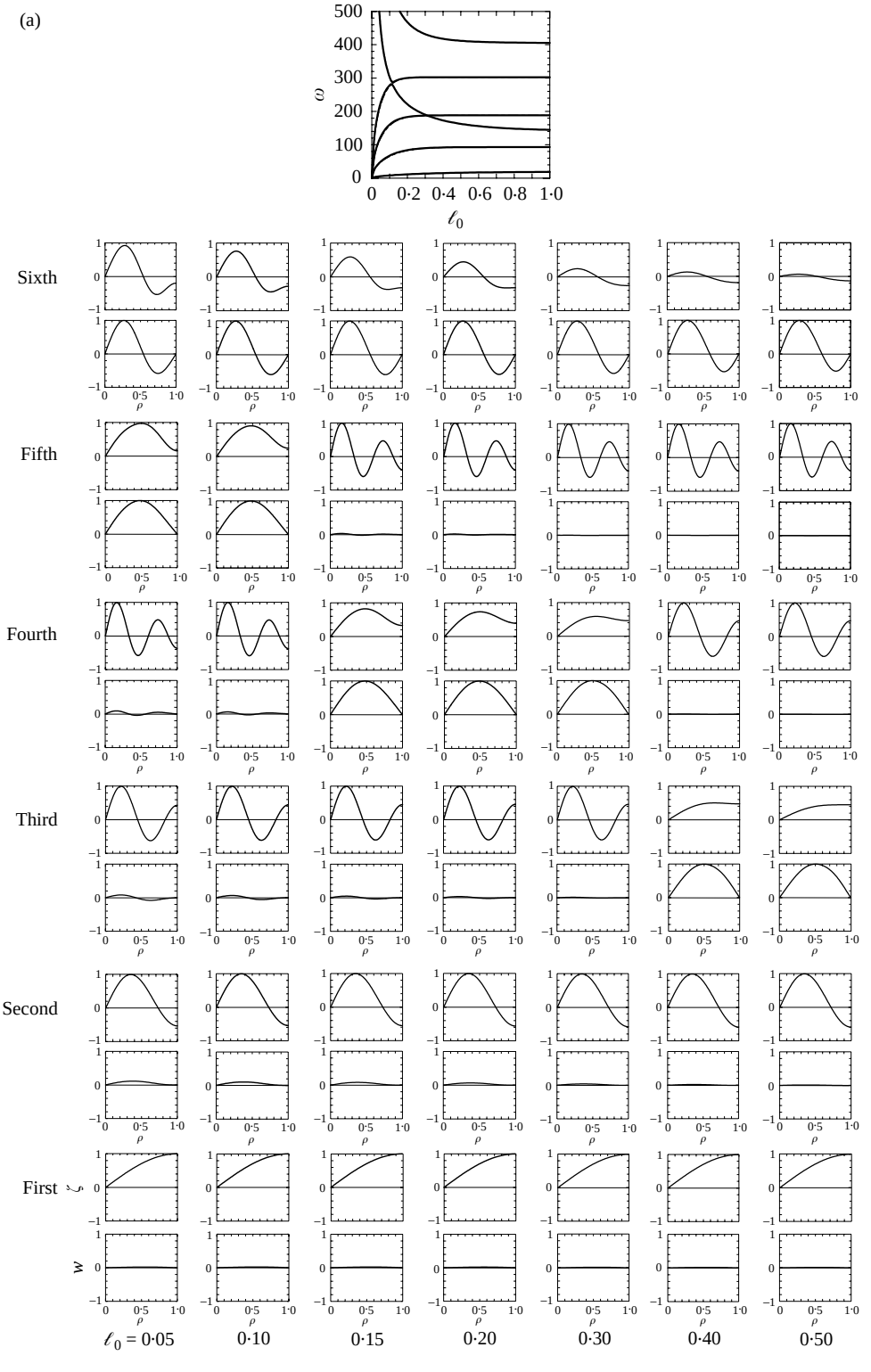

Figure 11. Coupled vibration modes for different liquid heights, ℓ_0, $m = 1$, $\bar{\rho} = 100$, $\bar{\sigma} = 100$, $\bar{T} = 10^5$: (a) slip, and (b) anchor.

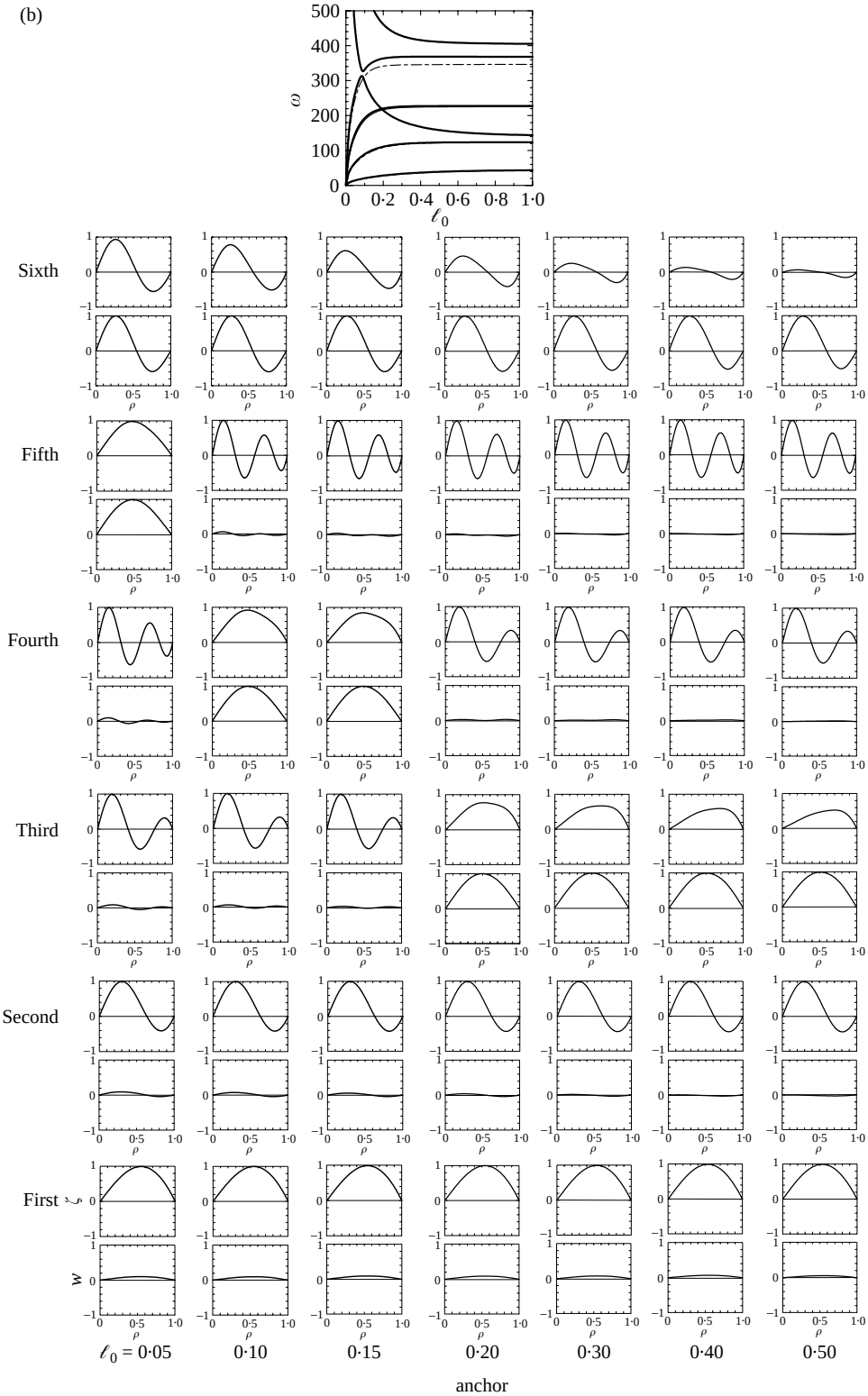

Figure 11. Continued

system can be obtained, however, by looking at the vibration modes. In Figure 11, vibration mode variations of the free surface and membrane are presented for some liquid heights ℓ_0 for the mode $m = 1$, the slip case (a) and the anchor case (b). In this figure, the vibration modes for the lowest six modes are presented, and the amplitude of the liquid free surface and the membrane are normalized to unity, from which we may recognize as to which of the motions is the predominant one.

For the case of slipping contact line, we notice from Figure 7(c) that both the first and second modes of sloshing and bulging are hardly interacting with each other. This may be observed by the fact that the mode shapes hardly do change, indicating only a weak coupling. This may be observed from Figure 11(a), where we find that the displacement of the membrane remains small for all the presented liquid height ratios ℓ_0. As soon as the bulging (membrane) frequency approaches the third sloshing mode frequency and coalesces with it near $\ell_0 \approx 0{\cdot}3$, both the bulging and sloshing mode exhibit large amplitudes and changed mode shapes.

Mode exchanges with liquid height ℓ_0 can clearly be observed, i.e., in both cases, the first and the second mode are the sloshing type, while the third mode changes from the sloshing type to the dominating bulging type as the liquid height ℓ_0 increases. And in the bulging mode, the magnitude of the liquid surface and membrane is of the same order if liquid height is small while the amplitude of the liquid surface becomes gradually smaller with the increase of ℓ_0. This may be seen in the sixth mode variations with ℓ_0. Similar results may be found for the case of an anchored contact line (Figure 11(b)), where the third mode shape change occurs at smaller ℓ_0.

4.3. AXISYMMETRIC VIBRATION WITH ANCHORED EDGE CONDITION

Finally, we shall see the effect of membrane tension $\bar{T}$ on the coupled vibration characteristics of the axisymmetric vibration $m = 0$ for the anchored edge condition. Figure 12(a) shows the coupled vibration frequency variations with $\bar{T}$, and Figure 12(b) shows the vibration modes when $\bar{T} = 7, 10, 30, 10^2, 500, 10^3, 10^4$, which are marked with circles in Figure 12(a). In Figure 12(a), the uncoupled sloshing frequencies are represented as dot–dashed lines, which represent horizontal lines. In the right-hand-side of the figure, their corresponding vibration modes are presented for reference. In a container with a rigid bottom or a container with high membrane tension $\bar{T}$, the lowest vibration mode is the $n = 2$ mode. With a decrease in membrane tension $\bar{T}$, the bulging-type natural frequencies gradually decrease and cross the sloshing natural frequency curves. It may be mentioned, that below the intersection point on the $\bar{T}$-axis of Figure 12(a), i.e., $\bar{T} = 3{\cdot}28$, the system becomes unstable. At this point the curve passes through zero frequency.

When we glance at Figure 12(a), two questions may arise. The first is why four nearly straight lines corresponding to the bulging natural frequencies turn into three lines after crossing the sloshing frequency curves with decrease in the membrane tension $\bar{T}$ from 10^6. The second is how to interpret the newly appearing horizontal line in the range of $\bar{T} = 1$–10, and $\omega \approx 9$. To answer these questions, we shall look at the vibration mode variations with $\bar{T}$, shown in Figure 12(b).

First, we look at the lowest vibration mode at $\bar{T} = 10^4$ and notice the sloshing mode with $n = 2$, which is the lowest one in a rigid bottom container. Then at $\bar{T} = 10^3$, movement of the bottom activates the liquid to vibrate with the mode $n = 1$ (due to the volume preserving condition), and the vibration mode seems either of bulging type with $n = 1$ or sloshing type with $n = 1$. A further decrease in $\bar{T}$ from 500 to 7, indicates a free surface amplitude decrease and a bottom mode change to the mode $n = 2$. These variations are schematically shown in

Figure 13 for a more obvious explanation. As the surface tension $\bar{\sigma}$ is of constant magnitude $\bar{\sigma} = 10$, flexibility of the membrane becomes relatively small in these ranges with small $\bar{T}$. When $\bar{T} = \infty$ or the container bottom is rigid, and free surface is "flexible" (Figure 13(a)), the mode $n = 1$ of the liquid free surface is impossible because of the volume conservation of the contained liquid. If the membrane tension $\bar{T}$ becomes small, the free surface tension appears relatively large (Figure 13(c)), which is a reverse situation from the case of Figure 13(a). Now the mode $n = 1$ of the bottom is impossible, which renders the disappearance of the bulging frequency curve with $n = 1$ at $\bar{T}$ of the small range in the ω–$\bar{T}$ diagram.

With decreasing membrane tension $\bar{T}$, we notice a change from small membrane motion (or zero membrane motion at $\bar{T} = \infty$) and large sloshing motion (for which the volume preserving condition demands the sloshing mode $n = 2$) to larger bottom motion and sloshing motion for the modes $n = 1$. This is again necessary to preserve the constant liquid volume condition. Finally, for very small membrane tension $\bar{T}$, the bottom has, due to the relatively large (stiff) liquid surface tension to move in the mode shape $n = 2$, while the liquid surface remains actually undisturbed. Similar effects may be concluded from higher modes, where we also observe phase jumps (Figure 12(b)).

Proceeding to the second question, we may recognize that the newly appeared horizontal line corresponds to the curve for sloshing frequency with $n = 1$ which cannot exist in a rigid

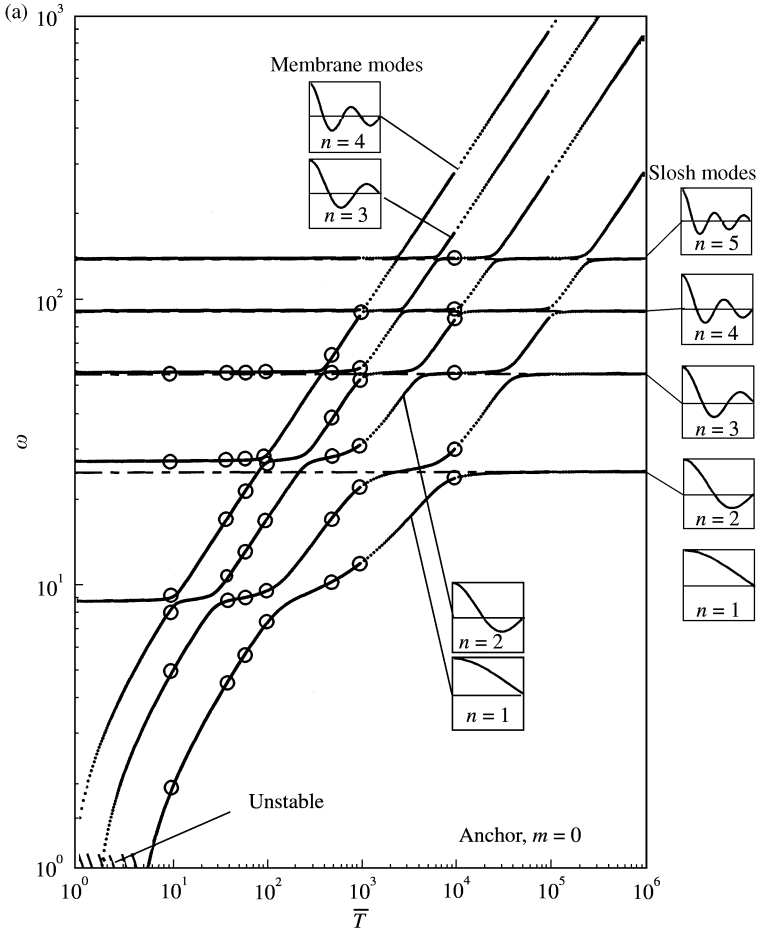

Figure 12. Effect of membrane tension $\bar{T}$ for anchored contact line, $m = 0$, $\bar{\rho} = 100$, $\bar{\sigma} = 10$, $\ell_0 = 0{\cdot}5$; (a) coupled natural frequency variation, and (b) vibration mode variation.

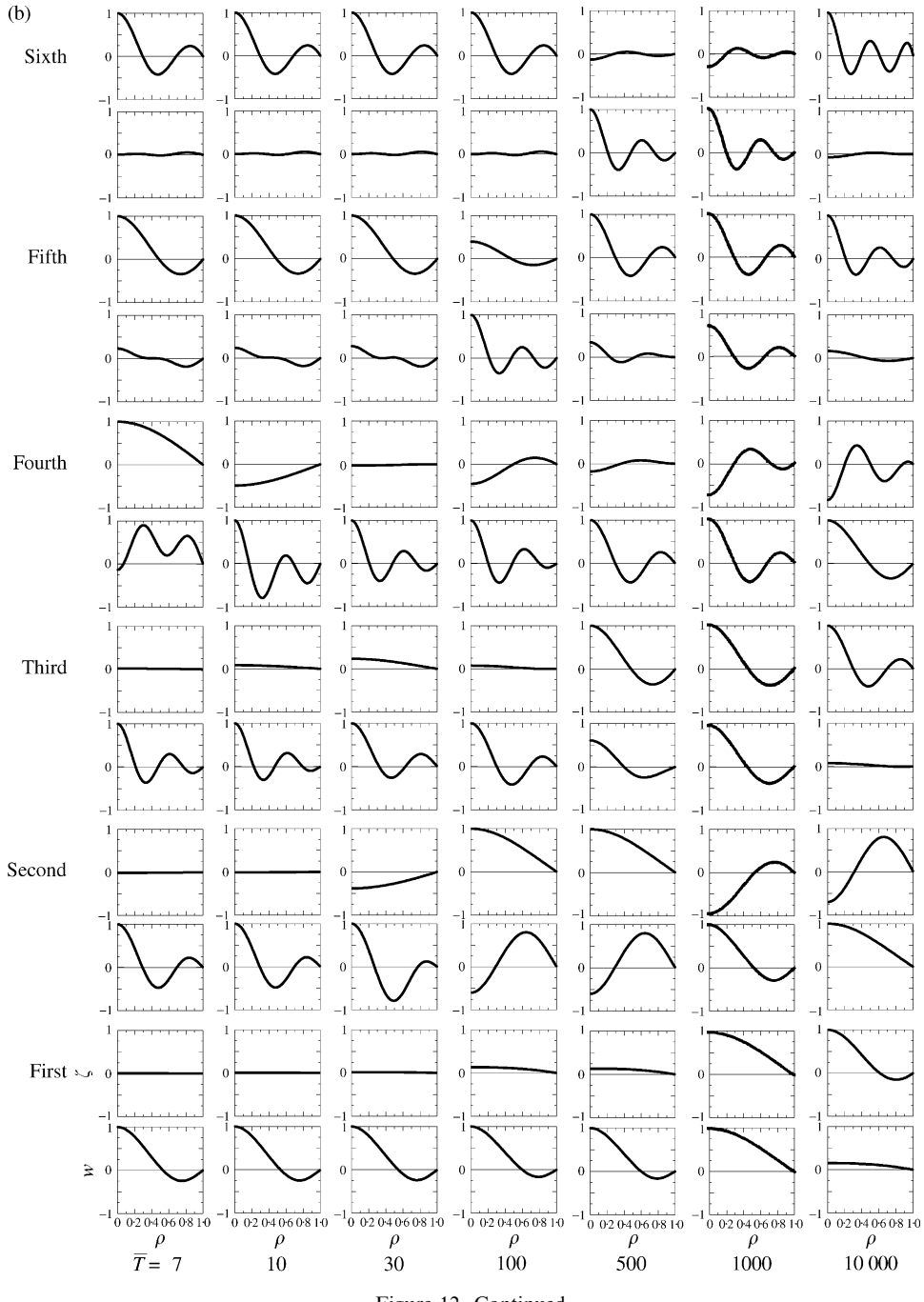

Figure 12. Continued.

bottom container. It should be noted that these phenomena are particular, since one just observes them in the axisymmetric vibration with anchored edge condition, and not in the asymmetric mode and slipping edge free surface condition.

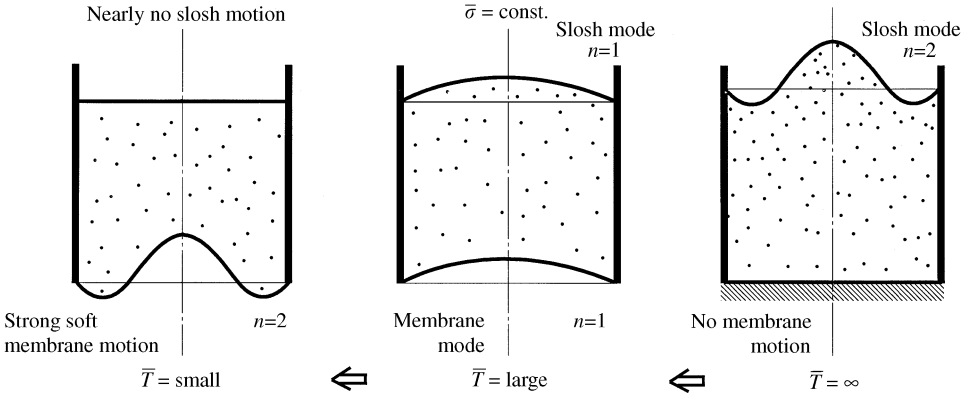

Figure 13. Coupled vibration mode variation with membrane tension $\bar{T}$.

Finally, it should be noted here that although it has been recognized from the previous studies that the flexibility of a bottom reduces sloshing natural frequency a little, in general, on the occasion when the coupling becomes strong, coupled sloshing natural frequencies are not always lower but lower or higher than those in a rigid bottom, depending on the coupling with bulging frequency. See the region at which two curves intersect each other without direct crossing but with indirect crossing, i.e., at $\omega = 25$ and $\bar{T} = 10^4$ in Figure 12(a).

5. CONCLUSION

Linear hydroelastic free vibration analysis of a cylindrical container with rigid side-wall and membrane bottom has been conducted with the inclusion of the effect of liquid free surface tension. Two types of liquid free surface edge conditions were considered. The main results as obtained from the present study are summarized as follows:

1. Coupling between membrane and liquid motion is pronounced by the reduction of the membrane tension $\bar{T}$, which reduces the bulging frequency, or by the increase in liquid surface tension, which increases sloshing frequency or both, and/or by the increase in mass ratio $\bar{\rho}$, which increases the added mass of the membrane and reduces the bulging frequency.
2. Uncoupled sloshing frequencies with an anchored edge condition are higher than those with slipping edge condition, the magnitude of the difference between the two becomes larger with the increase of surface tension $\bar{\sigma}$.
3. Influence of the difference of the two free surface edge conditions on the coupled bulging frequencies is negligibly small.
4. When the coupling between membrane and liquid motion becomes strong, coupled bulging and sloshing frequencies are of the same order. In such a case, the coupled sloshing frequency is either higher or lower than that of uncoupled sloshing frequency, depending on the influence of neighboring coupled bulging frequencies.
5. In the axisymmetric vibration with an anchored edge free surface condition, some interesting phenomena were found. When the membrane tension $\bar{T}$ is reduced from infinity, the lowest sloshing mode with $n = 2$ is changed to the mode $n = 1$ which can

appear only in a flexible bottom container. Further decrease in $\bar{T}$ makes the mode $n = 1$ of the membrane bottom disappear. In the region of small membrane tension $\bar{T}$, the coupled sloshing mode with $n = 1$ reappears.

6. Coupled bulging frequencies can be approximated by the membrane frequencies taking account of the effect of the (non-sloshing) liquid mass especially for the lowest mode with $n = 1$.

REFERENCES

1. P. G. Bhuta and L. R. Koval 1964 *Zeitschrift für Angewandte Mathematik und Physik* **15**, 466–480. Coupled oscillations of a liquid with a free surface in a tank having a flexible bottom.
2. P. G. Bhuta and L. R. Koval 1964 *Journal of the Acoustical Society of America* **36**, 2071–2079. Hydroelastic solution of the sloshing of a liquid in a cylindrical tank.
3. P. Tong 1967 *American Institute of Aeronautics and Astronautics Journal* **5**, 1842–1848. Liquid motion in a circular cylindrical container with a flexible bottom.
4. J. Siekmann and S.-C. Chang 1967 *Journal of Astronautical Sciences* **14**, 167–172. On liquid sloshing in a cylindrical tank with a flexible bottom under strong capillary and weak gravity conditions.
5. J. Siekmann and S.-C. Chang 1968 *Ingenieur-Archiv* **37**, 99–109. On the dynamics of liquids in a cylindrical tank with a flexible bottom.
6. H. F. Bauer, T.-H. Hsu and J. T.-S. Wang 1968 *Journal of Basic Engineering, Transactions of American Society of Mechanical Engineers* **68**, 1–5. Interaction of a sloshing liquid with elastic containers.
7. H. F. Bauer and J. Siekmann 1969 *Zeitschrift für Angewandte Mathematik und Mechanik* **49**, 577–589. Note on linear hydroelastic sloshing.
8. H. F. Bauer, J. T.-S. Wang and P. Y. Chen 1972 *Aeronautical Journal* **5**, 704–712. Axisymmetric hydroelastic sloshing in a circular cylindrical container.
9. M. Chiba 1993 *Journal of Fluids and Structures* **7**, 57–73. Non-linear hydroelastic vibration of a cylindrical tank with an elastic bottom, containing a liquid. Part II: linear axisymmetric analysis.
10. M. Chiba 1994 *Journal of Sound and Vibration* **169**, 387–394. Axisymmetric free hydroelastic vibration of a flexural bottom plate in a cylindrical tank supported on an elastic foundation.
11. H. F. Bauer 1999 *Forschungsberichte, Bundeswehr München*, LRT-WE-9-FB-1. Oscillations of non-viscous liquid in various containers.
12. M. Amabili, M. P. Paidoussis and A. A. Lakis 1998 *Journal of Sound and Vibration* **213**, 259–299. Vibrations of partially filled cylindrical tanks with ring-stiffeners and flexible bottom.
13. M. Chiba 1996 *International Journal of Non-linear Mechanics* **31**, 155–165. Non-linear hydroelastic vibration of a cylindrical tank with an elastic bottom containing liquid-III. Nonlinear analysis with Ritz averaging method.
14. M. Chiba and K. Abe 1999 *Thin-Walled Structure* **34**, 233–260. Nonlinear hydroelastic vibration of a cylindrical tank with an elastic bottom containing liquid-analysis using harmonic balance method.
15. M. Chiba 1997 *Journal of Sound and Vibration* **202**, 417–426. The influence of elastic bottom plate motion on the resonant response of a liquid free surface in a cylindrical container: a linear analysis.

APPENDIX A: NOMENCLATURE

a	radius of cylindrical container
A_0, B_0, A_{0n}, B_{0n}	unknown coefficients in equation (10)
A_{mn}, B_{mn}	unknown coefficients in equation (11)
Bo	Bond number ($Bo \equiv \rho_f g a^2/\sigma$)
c	parameter in equation (8)
g	gravitational acceleration
h	liquid height ($\ell_0 \equiv h/a$)
I_m	modified Bessel function of order m and first kind

i	imaginary unit
J_m	Bessel function of order m and first kind
m	circumferential vibration mode number
r, θ, z	polar co-ordinate system (ρ, θ, ξ), see equation (8)
T	tension of membrane ($\bar{T} \equiv T/ag\rho_m$)
t	time ($\tau = \Omega_0 t$), see equation (8)
w	membrane displacement ($w = W/a$)
β_{mn}	roots of $J_m(\beta) = 0$
Γ	liquid surface displacement ($\zeta = \Gamma/a$)
δ_{ns}	Kronecker's delta
ε_{mn}	roots of $J'_m(\varepsilon) = 0$
ρ_f	mass density of liquid
ρ_m	mass per unit area of membrane ($\bar{\rho} \equiv a\rho_f/\rho_m$)
σ	surface tension of liquid ($\bar{\sigma} \equiv \sigma/a^2 g\rho_f \equiv 1/Bo$)
Φ	velocity potential (ϕ)
Ω	coupled natural frequency ($\omega = \Omega/\Omega_0$: $\Omega_0^2 \equiv gc/a$)
$\omega^{(m)}$	uncoupled natural frequency of membrane
$\omega^{(ma)}$	coupled natural frequency of membrane with added (non-sloshing) liquid mass
$\omega^{(l)}$	uncoupled natural frequency of liquid